buildings

MDPI

Article

Influence Mechanism of Performance and Aging Behavior of High-Content SBS-Modified Asphalt

Qi Zheng [1], Haibo Wang [1], Beirong Jiang [1], Shulin Yue [2] and Tao Wang [2,*]

[1] School of Civil Engineering and Architecture, Hebei University of Engineering Science, Shijiazhuang 050091, China; zhengqi0726@163.com (Q.Z.)
[2] Department of Highway and Railway Engineering, School of Civil Engineering, Beijing Jiaotong University, Beijing 100044, China
* Correspondence: wangtao1@bjtu.edu.cn

Abstract

To address the research bottlenecks in the performance mechanism and engineering application of high-content SBS-modified asphalt (SBS content $\geq$ 6%), this study used 70# and 90# base asphalts as raw materials to prepare modified asphalts with SBS contents of 5%, 8%, 10%, and 12% via a high-speed shearing-stirring process. Combined with conventional performance tests (penetration, ductility, elastic recovery), rheological analysis (dynamic shear rheology (DSR), rotational viscosity), and micro-characterization (Scanning Electron Microscopy (SEM), X-ray photoelectron spectroscopy (XPS)), the regulatory mechanisms of SBS content, base asphalt type, and aging process (RTFOT short-term aging, PAV long-term aging) on asphalt performance were systematically investigated. The results showed that with the increase in SBS content, the asphalt's increased consistency (as indicated by decreased penetration), low-temperature crack resistance (5 °C ductility increased by more than 5 times), and high-temperature rutting resistance (60 °C complex shear modulus G* increased by 17 times) were significantly enhanced. Due to its higher content of light components, the 90# base asphalt exhibited a better modification effect than the 70# base asphalt. At 12% SBS content, the 5 °C ductility and 60 °C G* of the 90# base asphalt system reached 49.42 cm and 41.62 kPa, respectively. High-content SBS optimized the viscoelastic balance of asphalt: the 70# base asphalt system with 10–12% SBS content showed a phase angle $\delta < 45°$ (elasticity-dominated), and the modified asphalt with 12% SBS content exhibited a decrease in fatigue factor (G*sinδ) after PAV aging, indicating excellent fatigue resistance stability. The aging process significantly increased asphalt viscosity (the viscosity of 70# base asphalt with 10% SBS increased by 242% after PAV aging at 135 °C), while high-content SBS inhibited aging deterioration—the penetration ratio of both systems exceeded 96% at 10% SBS content. At the microscale, 10% SBS content enabled the asphalt to form a continuous and dense network structure, reducing carbon loss and slowing oxygen incorporation. Based on PG classification, the modified asphalt with 12% SBS content reached the PG100 grade, which can meet the needs of heavy-load and high-temperature scenarios such as high-toughness ultra-thin asphalt wearing courses. This study provides a key theoretical basis and data support for the content design and engineering promotion of high-content SBS-modified asphalt.

Keywords: high-content SBS-modified asphalt; aging behavior; rheological properties; microstructure

check for updates

Academic Editor: Nicolas Ali Libre

Received: 30 October 2025
Revised: 27 November 2025
Accepted: 3 December 2025
Published: 8 December 2025

Citation: Zheng, Q.; Wang, H.; Jiang, B.; Yue, S.; Wang, T. Influence Mechanism of Performance and Aging Behavior of High-Content SBS-Modified Asphalt. *Buildings* **2025**, *15*, 4430. https://doi.org/10.3390/buildings15244430

Copyright: © 2025 by the authors. Licensee MDPI, Basel, Switzerland. This article is an open access article distributed under the terms and conditions of the Creative Commons Attribution (CC BY) license (https://creativecommons.org/licenses/by/4.0/).

1. Introduction

High-content SBS-modified asphalt (SBS content $\geq$ 6%) is emerging as a crucial direction in the development of modified asphalt technology, owing to its significantly improved high- and low-temperature performance as well as anti-aging capacity [1]. It exhibits unique advantages, particularly in the application of high-toughness, ultra-thin asphalt wearing courses. As a special pavement structure typically with a thickness ranging from 1.5 to 2.5 cm, ultra-thin wearing courses impose extremely stringent requirements on the mechanical properties, bonding performance, and durability of materials. High-content SBS-modified asphalt not only provides sufficient shear strength to resist vehicle load effects but also effectively alleviates stress concentration in the thin-layer structure through its excellent elastic recovery capability, thereby extending the service life [2]. More importantly, the high-viscosity characteristic of this material enables it to form a good match with the ultra-thin structure, ensuring outstanding functional performance such as anti-slip and noise reduction even within the limited thickness [3].

At present, the relationships between very high SBS content ($\geq$6%), the resulting phase structure of asphalt, and its ultimate road performance are not yet fully understood—a critical gap that distinguishes high-content SBS-modified asphalt from conventional road-use SBS-modified asphalt (typically 3–5% SBS). In-depth research on high-content SBS-modified asphalt remains insufficient, despite its growing application potential [4]. Compared with conventional modified asphalt, high-content SBS-modified asphalt possesses superior high- and low-temperature performance as well as high viscosity. With the expanding application of new-type asphalt materials, high-content SBS-modified asphalt has also been gradually applied in new asphalt-based materials such as porous asphalt pavements, stress-absorbing layers, and waterproof materials [5]. In the long run, the market demand for high-content SBS-modified asphalt will continue to grow [6].

The Florida Department of Transportation (FDOT) conducted research on PG82-22 modified asphalt with a higher SBS content. Accelerated loading tests were mainly used to evaluate the rutting resistance of PG82-22 modified asphalt mixtures, while indirect tensile tests were employed to assess the fatigue performance of the mixtures [7]. The results showed that PG82-22 asphalt exhibited excellent actual road performance, and FDOT recommended that the Florida authorities promote the application of this type of asphalt when appropriate. Btazejowski evaluated the performance of a series of High-Content Polymer Modified Asphalts (HCPMAs) in Europe (with SBS content above 7%). The evaluation contents included, but were not limited to, the three key indicators (penetration, ductility, and softening point), asphalt cohesion, asphalt adhesion, resilience rate, high-temperature deformation resistance, medium-temperature fatigue resistance, and long-term thermal storage stability of asphalt. Laboratory studies indicated that all aspects of HCPMA performance were significantly superior to those of conventional modified asphalt [8].

The aging response of high-content SBS-modified asphalt differs significantly from that of base asphalt. Zhang et al. analyzed the effect of aging on the low-temperature properties of modified asphalt using Dynamic Shear Rheology (DSR) [9]. Lin et al. compared the variation patterns of complex modulus and phase angle of modified asphalt and base asphalt before and after aging and found that the phase angle of high-content SBS-modified asphalt did not decrease after aging but even increased to a certain extent [10]. Moreover, the higher the test temperature, the more obvious the increase, indicating that High-Content Polymer Modified Asphalt (HCPMA) exhibited a higher proportion of viscous response after aging. Airey conducted Rolling Thin Film Oven Test (RTFOT) aging and Pressure Aging Vessel (PAV) aging on high-content modified asphalt and obtained similar results. Cuciniello even observed a decrease in the modulus of HCPMA after aging, indicating an

unusually high value reduction in the high-temperature deformation resistance of HCPMA post-aging [11].

Modulus and phase angle are effective indicators that can directly reflect the viscoelastic properties of materials. In the field of modified asphalt aging research, researchers often use the Time-Temperature Superposition Principle (TTSP) to combine modulus data at different temperatures and evaluate the changes in the rheological properties of asphalt before and after aging in the form of master curves [12,13]. Li et al. prepared high-content SBS-modified asphalt using 8 different types of base asphalt, subjected them to thermo-oxidative aging, and explored the relationships between the composition and physical properties of base asphalt and the physical properties and aging performance of high-content SBS-modified asphalt [14]. The results showed that there was no correlation between the high- and low-temperature properties of base asphalt and those of high-content SBS-modified asphalt; the four components of base asphalt had a strong correlation with the low-temperature performance of high-content SBS-modified asphalt—base asphalt with higher saturate content and lower asphaltene content yielded high-content SBS-modified asphalt with better low-temperature flexibility, and base asphalt with a larger number of aromatic rings resulted in high-content SBS-modified asphalt with better anti-aging performance [15].

Li et al. conducted aging tests on high-content SBS-modified asphalt and 70# base asphalt, respectively, and carried out asphalt rheological performance tests. They evaluated the elastic recovery performance, high-temperature deformation resistance, and fatigue performance of high-content SBS-modified asphalt before and after aging, as well as the high-temperature stability, rutting resistance, and crack resistance of its mixture pre- and post-aging [16]. The research results indicated that with the deepening of aging degree, the modulus of high-content SBS-modified asphalt increased, while its elastic recovery performance, high-temperature deformation resistance, and fatigue performance weakened; meanwhile, the high-temperature stability and high-temperature deformation resistance of the mixture decreased, and the crack resistance gradually deteriorated [17].

At present, medium- and high-content SBS-modified asphalt has attracted widespread attention from domestic and foreign scholars, but the modifier content is mostly within 8%. There are a few systematic studies on asphalt modified with 10% and 12% SBS. In this study, a gradient of SBS contents (5–12%) was designed to conduct systematic research on the performance and aging behavior of high-content SBS-modified asphalt. Using 70# and 90# base asphalts as raw materials, a series of high-content SBS-modified asphalts were prepared by adding SBS modifier at different contents (5%, 8%, 10%, 12%), aiming to systematically explore the influence of the law of SBS content on the basic properties and rheological behavior of asphalt materials. The focus of this study is not on the marginal improvement of performance by a small amount of modifier but on revealing the synergistic enhancement mechanisms of asphalt materials in terms of high- and low-temperature mechanical properties, aging behavior, and viscoelastic characteristics under high-content SBS modification.

2. Materials and Methods

2.1. Raw Materials

2.1.1. Base Asphalt

The base asphalts used were 70# and 90# petroleum asphalt (Batch No.: DM20230512 for 70#, DM20230515 for 90#) produced by Dongming Petrochemical Co., Ltd. (Heze, China). Prior to use, all base asphalt was stored in a sealed iron drum at 25 ± 2 °C for 72 h to eliminate thermal stress from transportation. A 500 g sample was taken from the middle layer of the drum (to avoid bottom sediment) and preheated at 160 ± 1 °C for 2 h

(forced-convection oven, Model: DHG-9075A, Shanghai Jinghong Laboratory Instrument Co., Ltd., Shanghai, China) to ensure uniform melting. Technical indicators were tested in triplicate (average values reported) in accordance with JTG E20-2011 Standard Test Methods of Bitumen and Bituminous Mixtures for Highway Engineering [18]. Results are shown in Table 1.

Table 1. Technical requirements for 70# and 90# Grade Petroleum Asphalt.

Test Items		70# Grade Petroleum Asphalt		90# Grade Petroleum Asphalt	
		Technical Requirements	Test Results	Technical Requirements [18]	Test Results
Penetration (0.1 mm) (25 °C, 100 g, 5 s)		60~80	64	80~100	88
Ductility (5 cm/min, 15 °C) (cm)		≥40	46.0	≥45	54
Softening point (°C)		>46	48.2	≥44	45.5
Density (15 min) (g/cm^3)		Actual measurement	1.01	Actual measurement	1.00
Solubility (%)		≥99.5	99.8	≥99	99.6
Wax content (Distillation) (%)		≤2.2	2.0	≤2	1.9
Dynamic Viscosity (60 °C) (Pa·s)		≥180	185.6	≥160	168.3
After aging in film ovens	Weight loss (%)	≤±0.8	**0.072**	≤±1	**0.067**
	Residual needle penetration ratio (%)	≥61	**65**	≥64	**67**
	Residual ductility (10 °C) (cm)	≥10	**12.5**	≥8	**9.2**

2.1.2. SBS Modifier

SBS modifier (Model: YH-791E, alias SBS 1301E; Batch No.: BL20230408) was supplied by Yueyang Baling Petrochemical Co., Ltd. (Yueyang, China). The modifier was in white strip form (length: 3 ± 0.5 cm, width: 1 ± 0.2 cm) and stored in a dry, cool warehouse (relative humidity: 40 ± 5%, temperature: 20 ± 2 °C) to prevent moisture absorption. Before use, the strips were crushed into 1–2 mm particles using a stainless steel crusher (Model: XF-100, Beijing Xinghua Instrument Co., Ltd., Beijing, China) to ensure rapid swelling in base asphalt. Key parameters (tested per GB/T 20674.1-2006 Styrene-Butadiene-Styrene Block Copolymer (SBS) for Rubber Modified Asphalt) are shown in Table 2 [19].

Table 2. SBS modifier parameters.

Item	YH-791E (SBS 1301E)
Manufacturer	Yueyang Baling Petrochemical Co., Ltd.
Structural type	Linear
Block ratio S/B	30/70
Oil filling rate (%)	0
Volatile matter (%)	≤0.7
Ash content (%)	≤0.2
300% tensile stress (MPa)	≥2
Tensile strength (MPa)	≥13
Elongation at break (%)	≥680
Permanent set (%)	≤40
Melt flow rate (g/10 min)	0.5~5

2.1.3. Stabilizers

The stabilizer was a sulfur-based yellow powder (purity: 99.5%, particle size: 200 mesh; Batch No.: LS20230320) supplied by Luoyang Sulfur Chemical Co., Ltd. (Luoyang, China). It was dried in a vacuum oven (Model: DZF-6050, Shanghai Yiheng Scientific Instrument Co., Ltd., Shanghai, China) at 80 ± 2 °C for 4 h to remove residual moisture (moisture content <0.1% after drying, tested via Karl Fischer titration, Model: KF-1A, Shanghai Precision Scientific Instrument Co., Ltd., Shanghai, China)—moisture was controlled to avoid bubble formation during asphalt preparation.

2.2. Preparation Process

Due to the high content of SBS, in order to ensure sufficient reflection between SBS and matrix asphalt, a high-speed shearing machine and mixer were used to prepare SBS-modified asphalt. The specific preparation process is shown in Figure 1.

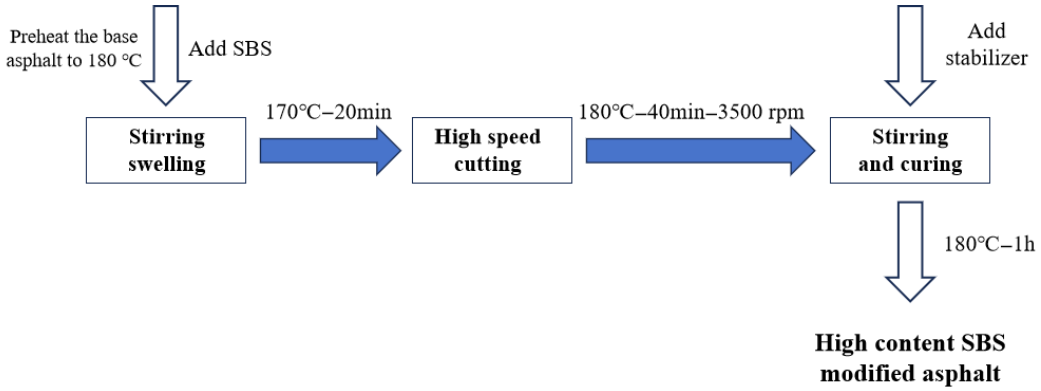

Figure 1. Preparation process of modified asphalt.

Due to the high content of SBS (5–12%), ensuring sufficient swelling, dispersion, and interfacial bonding between SBS and base asphalt requires precise control of processing parameters. A high-shear mixer (Model: HSM-100, Shanghai Likang Instrument Co., Ltd., Shanghai, China) and thermostatic magnetic stirrer (Model: DF-101S, Gongyi Yuhua Instrument Co., Ltd., Henan, China) were used for preparation, with strict thermal history control (all specimens underwent identical temperature-time protocols to avoid differential pre-aging). The key parameters are summarized in Table 3.

Table 3. Detailed preparation parameters for high-content SBS-modified asphalt (with standard references).

Preparation Step	Equipment Model/Type	Key Parameters	Purpose
Base asphalt preheating	Forced-convection oven (DHG-9075A)	160 °C, 2 h; 180 °C, 30 min (±1 °C)	Uniform melting, no pre-aging
Preliminary mixing	Magnetic stirrer (DF-101S)	Paddle impeller (45°), 500 rpm, 20 min	SBS wetting/swelling, no agglomeration
High-speed shearing	High-shear mixer (HSM-100)	Serrated titanium rotor, 3500 rpm, 0.5 mm shear gap, 40 min	Uniform SBS dispersion, network formation
Stabilizer curing	Magnetic stirrer (DF-101S)	500 rpm, 180 °C, 60 min	Cross-linking, stable network
Thermal history control	Thermostatic chamber (BPH-9162)	Natural cooling to 60 °C, same batch processing	Consistent thermal conditions across specimens

(1) Base asphalt preheating. Place 500 g of 70#/90# base asphalt in a 1000 mL cylindrical container and heat in a forced-convection oven at 160 °C for 2 h (to melt uniformly without light component volatilization, verified by constant mass measurement). Transfer to a thermostatic electric heating jacket (±1 °C temperature accuracy) and raise the temperature to 180 °C; maintain for 30 min to stabilize the temperature (avoid local overheating).

(2) SBS addition and preliminary mixing. Add the pre-weighed SBS modifier (5%/8%/10%/12% of base asphalt mass) to the 180 °C base asphalt. Use a magnetic stirrer (impeller type: paddle-shaped, 45° inclination; rotational speed: 500 rpm) for 20 min—this low-speed mixing ensures SBS is fully wetted and swollen (prevents agglomeration) without inducing shear degradation.

(3) High-speed shearing. Maintain the temperature at 180 °C (monitored by a K-type thermocouple inserted 2 cm below the asphalt surface). Use the high-shear mixer with a

titanium alloy rotor (serrated structure, diameter: 30 mm) at a rotational speed of 3500 rpm for 40 min. The shear gap (rotor-stator distance) was fixed at 0.5 mm to ensure uniform shear intensity across all specimens; the container was wrapped in thermal insulation cotton to minimize temperature fluctuations (<±2 °C).

(4) Stabilizer addition and curing. Add the stabilizer (sulfur-based, purity: 99.5%)—dosage: 0.25% (5% SBS), 0.4% (8%/12% SBS), or 0.5% (10% SBS) of total asphalt mass. Continue stirring at 180 °C with the magnetic stirrer (500 rpm) for 60 min to promote cross-linking between SBS and sulfur (curing) while avoiding over-curing (verified by constant viscosity measurement at 135 °C).

(5) Thermal history control. All specimens (regardless of SBS content) were processed in the same batch, with identical heating rates (5 °C/min from 160 °C to 180 °C), holding times, and cooling protocols (natural cooling to 60 °C in a thermostatic chamber before performance testing). A blank control test (base asphalt heated at 180 °C for 120 min) confirmed no significant pre-aging: the penetration ratio (vs. unheated base asphalt) was 98.2% (70#) and 97.8% (90#), well above the 80% threshold for negligible pre-aging.

High-content SBS-modified asphalts with SBS contents of 5%, 8%, 10%, and 12% were prepared, respectively. Among them, due to the excessively high viscosity of the 12% SBS-modified asphalt, the dosage of the stabilizer was set to 0.4%. For the modified asphalts with 5%, 8%, and 10% SBS contents, the dosage of the stabilizer was 5% of the SBS content. The specific proportions are shown in Table 4.

Table 4. Different types of asphalt formulas.

Asphalt Type	Binder	SBS Modifier	Stabilizer
5%SBS	94.75%	5%	0.25%
8%SBS	91.6%	8%	0.4%
10%SBS	89.5%	10%	0.5%
12%SBS	87.6%	12%	0.4%

2.3. Experimental Methods

2.3.1. Penetration Test

The penetration test was conducted. Heat the modified asphalt to 135 ± 5 °C (to avoid overheating) and pour it into a standard penetration cup (diameter: 55 mm, height: 35 mm) to a depth of 25 ± 1 mm. Cool in a water bath at 25 ± 0.1 °C for 1.5 h; level the surface with a hot knife (temperature: 60 ± 5 °C) 15 min before testing. Test parameters: Use a standard penetration needle (length: 50 ± 1 mm, diameter: 1.00 ± 0.05 mm, mass: 50 ± 0.05 g) with a total load of 100 ± 0.1 g (needle + weight). Lower the needle to contact the sample surface (no pressure applied), then release for 5 ± 0.1 s; record the penetration depth (unit: 0.1 mm) via the digital display (accuracy: 0.01 mm, Model: LPN-100, Shanghai Liangpu Instrument Co., Ltd.). Replicates and calculation: Test 3 parallel samples per asphalt type (each sample tested at 3 different positions, 9 data points total); remove outliers (Grubbs test, significance level $\alpha = 0.05$) and calculate the average. For aged samples (RTFOT), the penetration ratio was calculated as (penetration after RTFOT/original penetration) × 100%, with RSD < 5%.

2.3.2. Ductility Test

The ductility test (stretching at 5 °C) quantifies the low-temperature crack resistance of asphalt by measuring the maximum tensile length (unit: cm) of an asphalt specimen before fracture at a specific temperature [19]. A high ductility value (e.g., >40 cm) indicates that asphalt can release stress through plastic deformation even at low temperatures, preventing the formation of pavement shrinkage cracks. The incorporation of SBS modifier significantly improves asphalt ductility, especially in the low-temperature range (e.g., −10 °C to 5 °C),

and the three-dimensional network structure formed by SBS effectively inhibits brittle fracture. This indicator provides key references for the design of low-temperature durability of asphalt used in cold-region pavements.

2.3.3. Elastic Recovery Test

The elastic recovery test (at 25 °C) evaluates the elastic deformation capacity of modified asphalt by measuring the deformation recovery ratio (unit: %) of an asphalt specimen after stretching and relaxation at room temperature. A high elastic recovery rate (e.g., >80%) indicates that asphalt can offset stress through elastic deformation under load, reducing the accumulation of pavement rutting and fatigue cracks [20]. The addition of the SBS modifier enhances the viscoelasticity of asphalt via a cross-linked polymer network, enabling the material to rebound rapidly in the medium-temperature range (25 °C) and avoid permanent deformation. This indicator offers important guidance for the anti-deformation design of pavements in high-temperature and rainy areas or under heavy traffic loads.

2.3.4. DSR Rheological Test

The DSR test was conducted using a dynamic shear rheometer, produced by TA Instruments, Newcastle, USA. Sample preparation: Heat the asphalt to 135 ± 5 °C and pour it into a 25 mm diameter aluminum mold; cool at 25 ± 2 °C for 1 h, then trim to a thickness of 1.0 ± 0.1 mm (for temperature sweep) or 2.0 ± 0.1 mm (for frequency sweep) using a precision cutter (Model: DSR-T01, Anton Paar GmbH, Graz, Austria).

(1) Temperature sweep test: Conducted within a temperature range of 52–100 °C (temperature interval of 6 °C) at a fixed frequency of 10 Hz and strain amplitude of 12%. The test parameters included complex modulus (G*) and phase angle (δ), aiming to evaluate the temperature sensitivity of viscoelastic properties under practical engineering strain conditions.

(2) Frequency sweep test: Performed to establish master curves based on the Time-Temperature Superposition Principle (TTSP). Tests were carried out at a strain amplitude of 1%, frequency sweep range of 0.1–20 Hz, and temperature range of 50 °C, 60 °C, 70 °C, and 80 °C.

Amplitude sweep verification (0.1–10% strain, 60 °C, 10 Hz) was conducted on all asphalt samples to determine the LVE range. The results showed that the strain threshold for LVE of unmodified asphalt was ~3%, while that of high-content SBS-modified asphalt (≥8% SBS) was ~5%. This confirmed that the 1% strain used in frequency sweep tests was strictly within the LVE range, ensuring the reliability of master curve data. In contrast, the 12% strain adopted in temperature sweep tests was intentionally selected to simulate the strain level of asphalt under actual vehicle loading [21], which exceeds the LVE threshold of unmodified asphalt.

Frequency sweep testing is a primary method for measuring the linear viscoelastic mechanical parameters of asphalt. Under a constant temperature, dynamic shear tests with small strain levels (1%, within LVE) and different loading frequencies were applied to specimens, allowing the acquisition of the dynamic mechanical response of asphalt within the linear viscoelastic range.

Subsequently, based on the frequency sweep results at different temperatures and combined with the Time-Temperature Superposition Principle (TTSP), the frequency sweep data at various temperatures were horizontally shifted to establish master curves for storage modulus, loss modulus, and dynamic modulus. The influence of the law of aging on the viscoelastic properties of asphalt specimens was quantitatively determined by analyzing the variation trend of the master curves.

2.3.5. Rotational Viscosity Test

The rotational viscosity test (using a Brookfield viscometer) measures the flow resistance (unit: Pa·s) of asphalt at 135 °C, 155 °C, 175 °C, and 180 °C, which is used to evaluate its workability and pumpability during construction [22]. Due to the polymer swelling effect, the viscosity of SBS-modified asphalt is significantly higher than that of base asphalt. Excessively high viscosity may cause segregation during paving; thus, this indicator provides direct guidance for determining mixing and compaction process parameters, as well as the application of warm-mix modification technology.

2.3.6. Scanning Electron Microscopy (SEM) Test

The SEM test was employed to observe the surface morphology and microstructural characteristics of SBS-modified asphalt at the microscale. High-resolution electron beam imaging enabled the analysis of the distribution state, compatibility, and structural continuity of the polymer (SBS) in the asphalt matrix under different SBS contents. With the increase in SBS content, more obvious network-like structures were observed in the asphalt, reflecting the phase separation behavior of the polymer and its skeleton-supporting effect. In addition, by comparing specimens under different aging states (original, RTFOT-aged, and PAV-aged), the destructive effect of aging on the microstructure and the variation law of polymer phase morphology were revealed. This test helps to understand the performance evolution mechanism of SBS-modified asphalt from a microscale perspective.

2.3.7. X-Ray Photoelectron Spectroscopy (XPS) Elemental Analysis

XPS elemental analysis was used to determine the surface elemental composition and chemical state of SBS-modified asphalt. By quantitatively analyzing the content changes in elements such as carbon (C), oxygen (O), and sulfur (S), the surface chemical characteristics of asphalt under different SBS contents and aging states could be reflected. XPS analysis directly reveals the chemical environment of different elements on the asphalt surface: for example, a decrease in C content and an increase in O content usually indicate that the asphalt has undergone oxidative aging; changes in S content help to understand the stability and variation in sulfides in the asphalt. By comparing XPS spectra under different aging states, researchers can reveal the surface chemical reaction pathways of SBS-modified asphalt (e.g., the reaction between oxygen and aromatic carbon or other functional groups in asphalt), thereby further analyzing the anti-aging performance and durability of SBS-modified asphalt.

3. Results and Discussion

3.1. Penetration Result

Penetration (25 °C) and penetration ratio (after RTFOT) were used to characterize asphalt's room-temperature hardness and anti-aging performance (Figure 2). In the original state, 70# and 90# base asphalts had penetrations of 60.6 and 75.2 (0.1 mm), respectively—reflecting the softer initial structure of 90# asphalt. With increasing SBS content (5–12%), penetrations of both systems decreased gradually: 70# asphalt dropped to 31.4 (0.1 mm) at 12% SBS, while 90# asphalt decreased to 29.2 (0.1 mm). This trend is attributed to the SBS-formed spatial network, which restricts molecular movement and enhances deformation resistance. After RTFOT aging, unmodified asphalts showed significant penetration reductions (70#: 40.1% reduction; 90#: 44.9% reduction), whereas high-content SBS mitigated this decline. For 10–12% SBS systems, penetration reductions were <4% (70#: 3.7–2.4 (0.1 mm); 90#: 3.0–2.1 (0.1 mm)), and penetration ratios exceeded 96% (vs. 55–59.9% for unmodified asphalts). Notably, 90#-based asphalt with 10% SBS exhibited a slightly higher penetration ratio (96.9%) than 70#-based asphalt (96.2%), confirming that high-content

SBS has a more pronounced anti-aging effect on softer base asphalts (due to better SBS dispersion in light components).

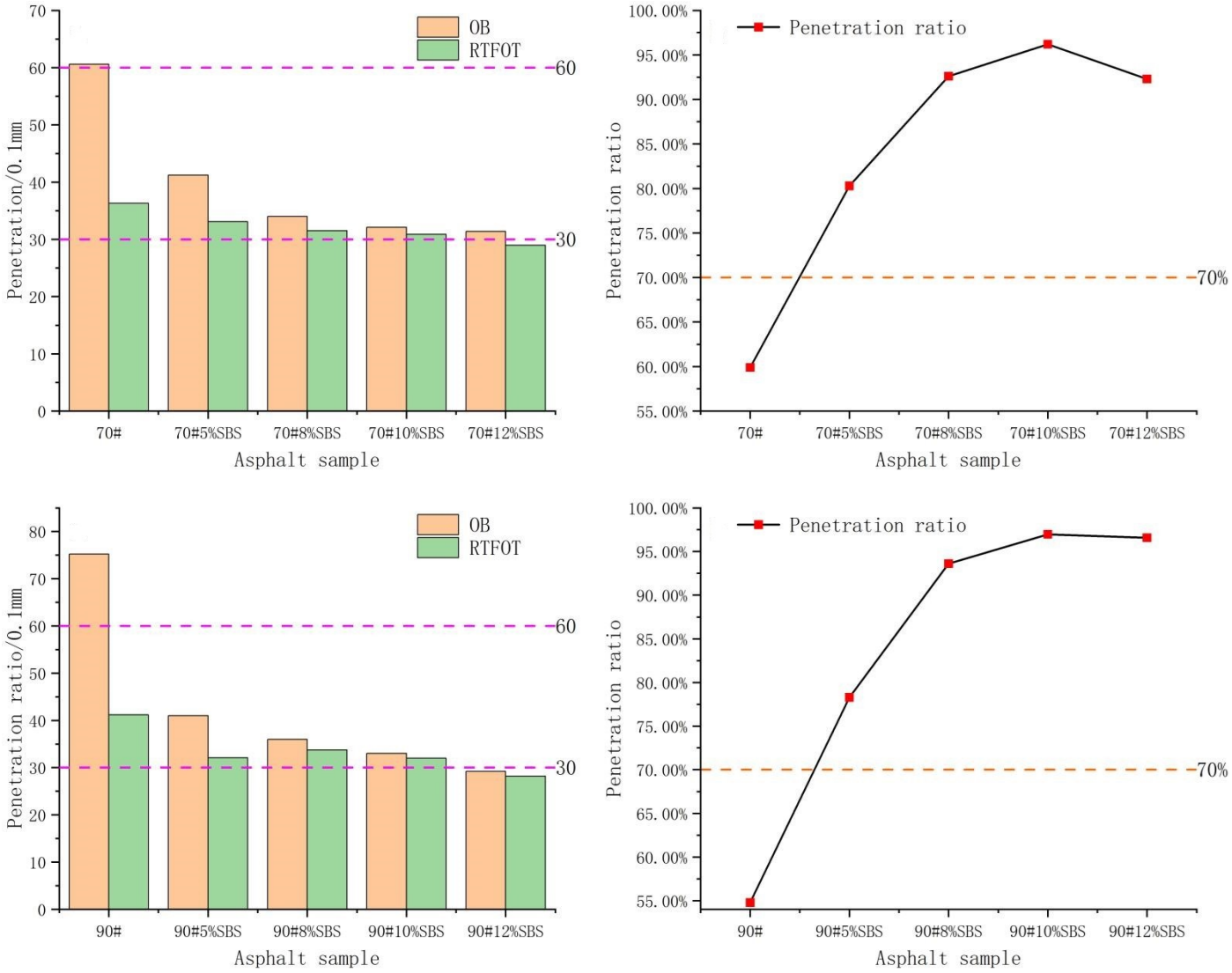

Figure 2. Penetration (**left**) and penetration ratio (**right**). (**top**) 70#binder; (**bottom**) 90# binder.

3.2. Ductility Result

Ductility (5 °C) quantified low-temperature crack resistance (Figure 3). Unmodified 70# and 90# base asphalts had ductilities of only 7.14 cm and 6.17 cm, respectively (brittle characteristics). With SBS addition, ductility increased significantly: at 12% SBS, 70#-based asphalt reached 40.87 cm (5.7× higher than base asphalt), while 90#-based asphalt reached 49.42 cm (8× higher than base asphalt). This improvement stems from the continuous elastic network of SBS, which inhibits microcrack propagation under tension. 90#-based asphalt exhibited higher ductility than 70#-based asphalt at all SBS contents, as its higher light component content facilitates SBS swelling and network formation. Per JTG F40-2004, 5–8% SBS-modified asphalt (both base types) meets Grade I-C, while 10–12% SBS systems meet Grade I-B—verifying their applicability in cold-region pavements.

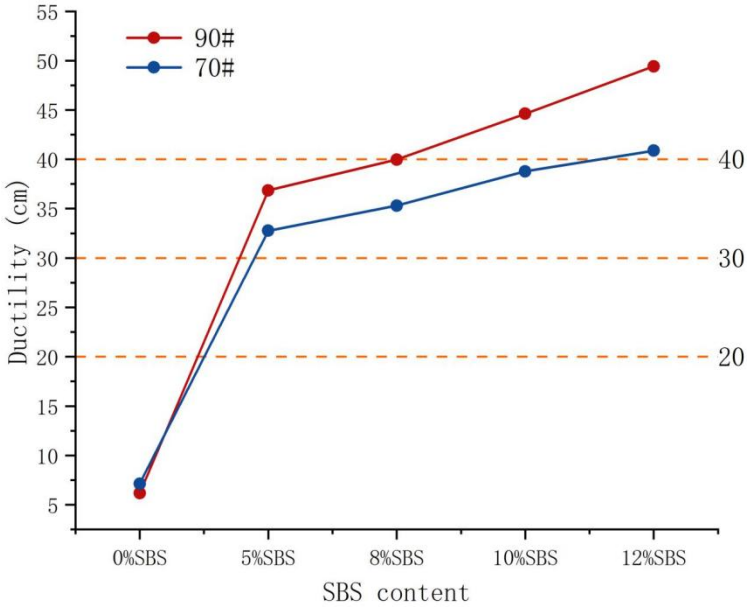

Figure 3. Ductility.

3.3. Complex Shear Modulus at 60 °C (G)*

The 60 °C complex shear modulus (G*) of modified asphalts with different SBS contents (0%, 5%, 8%, 10%, 12%) was measured in both the original state (OB) and after RTFOT aging to explore the influence mechanisms of SBS content, aging process, and base asphalt type on the high-temperature deformation resistance of asphalt. The result is shown in Figure 4.

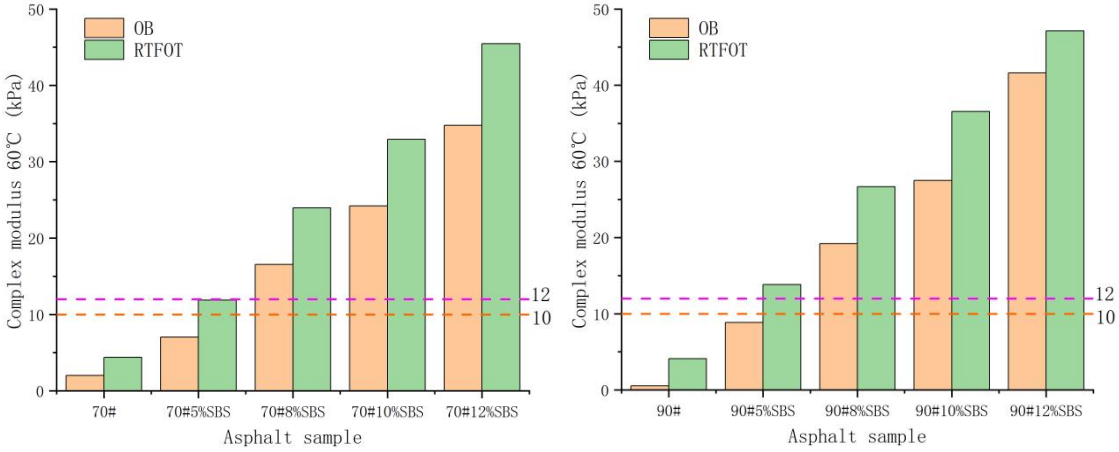

(**a**) 70# type (**b**) 90# type

Figure 4. 60 °C complex shear modulus of SBS-modified asphalt.

The test results showed that the 60 °C G* of both types of base asphalt increased significantly with the increase in SBS content, and G* further increased after aging. For the 70# base asphalt, the G* in the OB state was only 2.00 kPa, which increased to 4.39 kPa after RTFOT aging (an increase of 119.5%). After incorporating 5%, 8%, 10%, and 12% SBS, the OB-state G* increased to 7.04 kPa, 16.55 kPa, 24.22 kPa, and 34.75 kPa, respectively; after RTFOT aging, the corresponding G* values reached 11.89 kPa, 23.96 kPa, 32.93 kPa, and 45.46 kPa. For the 90# base asphalt, the OB-state G* was 0.53 kPa (only 26.5% of that of the 70# base asphalt), which surged to 4.11 kPa after RTFOT aging (an increase of 775%). Under the same SBS content, the OB-state G* of the 90#-based modified asphalt was 8.85 kPa, 19.21 kPa, 27.51 kPa, and 41.62 kPa, respectively; after RTFOT aging, the values reached

13.84 kPa, 26.68 kPa, 36.55 kPa, and 47.14 kPa, with the highest G* across all samples observed at 12% SBS content.

The three-dimensional elastic network structure formed by SBS in asphalt can significantly enhance the shear resistance at high temperatures. During aging, the volatilization of light components and molecular cross-linking reactions further strengthen the network stiffness, thus leading to an increase in G* after aging. Although the 90# base asphalt had a low initial G*, its high content of light components facilitated the dispersion of SBS segments and the formation of the network structure. As a result, the G* of the 90#-based system exceeded that of the 70#-based system at high SBS contents (≥8%), demonstrating the synergistic enhancement effect of "soft base asphalt + high-content SBS".

3.4. Temperature Sweep

1. Complex Modulus (G*)

DSR temperature sweeps (52–100 °C) characterized G* (deformation resistance) and δ (viscoelastic balance) under original (OB), RTFOT, and PAV aging states (Figure 5).

The test results showed that in the low-temperature range (52–58 °C), the G* of unmodified 70# base asphalt was higher than that of 90# base asphalt, indicating that 70# base asphalt inherently has better deformation resistance. However, after incorporating SBS, the increase in G* of the 90#-based system was significantly greater than that of the 70#-based system: at 5% SBS content, the G* of 90#-based asphalt exceeded that of 70#-based asphalt in the 52–58 °C range; the gap further widened when the SBS content was ≥ 8%; and at 10% SBS content, the G* of 90#-based modified asphalt was significantly higher than that of 70#-based modified asphalt across the entire 52–94 °C range. For both types of base asphalts, the G* of modified asphalts increased with the increase in SBS content, reaching a peak at 12% SBS content. The modification effect was more pronounced in the high-temperature range (≥76 °C), confirming that the three-dimensional network structure formed by high-content SBS effectively inhibits high-temperature deformation.

The influence of aging on G* was dependent on the type of base asphalt. For unmodified asphalts, 90# base asphalt (with a higher content of light components) exhibited a greater increase in G* than 70# base asphalt after RTFOT aging; however, after PAV aging, the G* of 90# base asphalt surpassed that of 70# base asphalt. This phenomenon is attributed to the fact that the aromatic components in 90# base asphalt are more prone to oxidation, leading to the formation of cross-linked structures. After incorporating SBS, the magnitude of the aging effect on G* gradually diminished with increasing SBS content. At 12% SBS content, the difference in G* changes between RTFOT and PAV aging narrowed, indicating that the high-content SBS network can inhibit aging-induced structural degradation.

Master curve analysis revealed that with increasing SBS content and aging degree, the master curves shifted upward vertically (indicating higher stiffness), and the slope in the high-frequency/low-temperature region decreased (indicating reduced temperature sensitivity). For the 70#-based system, the G* values at 8% and 10% SBS contents were similar, while a significant increase was observed when the SBS content increased from 10% to 12%. For the 90#-based system, the largest increase in G* occurred between 8% and 10% SBS content, and the increase slowed down between 10% and 12% SBS content. These results reflect the differences in the synergistic effect thresholds between the two types of base asphalts and SBS, providing a micromechanical basis for the design of asphalt SBS content under different climatic and loading conditions.

2. Phase Angle (δ)

Phase angle (δ) reflects the viscoelastic balance of asphalt (Figure 6): $\delta < 45^\circ$ indicates elasticity-dominated behavior (excellent fatigue resistance, critical for medium-temperature heavy-load scenarios), while $\delta > 45^\circ$ indicates viscosity-dominated behavior (excellent

rutting resistance, key for high-temperature scenarios). For the study's target applications—high-toughness ultra-thin wearing courses (requiring both rutting resistance and fatigue crack resistance) and cold-region pavements (needing low-temperature crack resistance alongside medium-temperature durability).

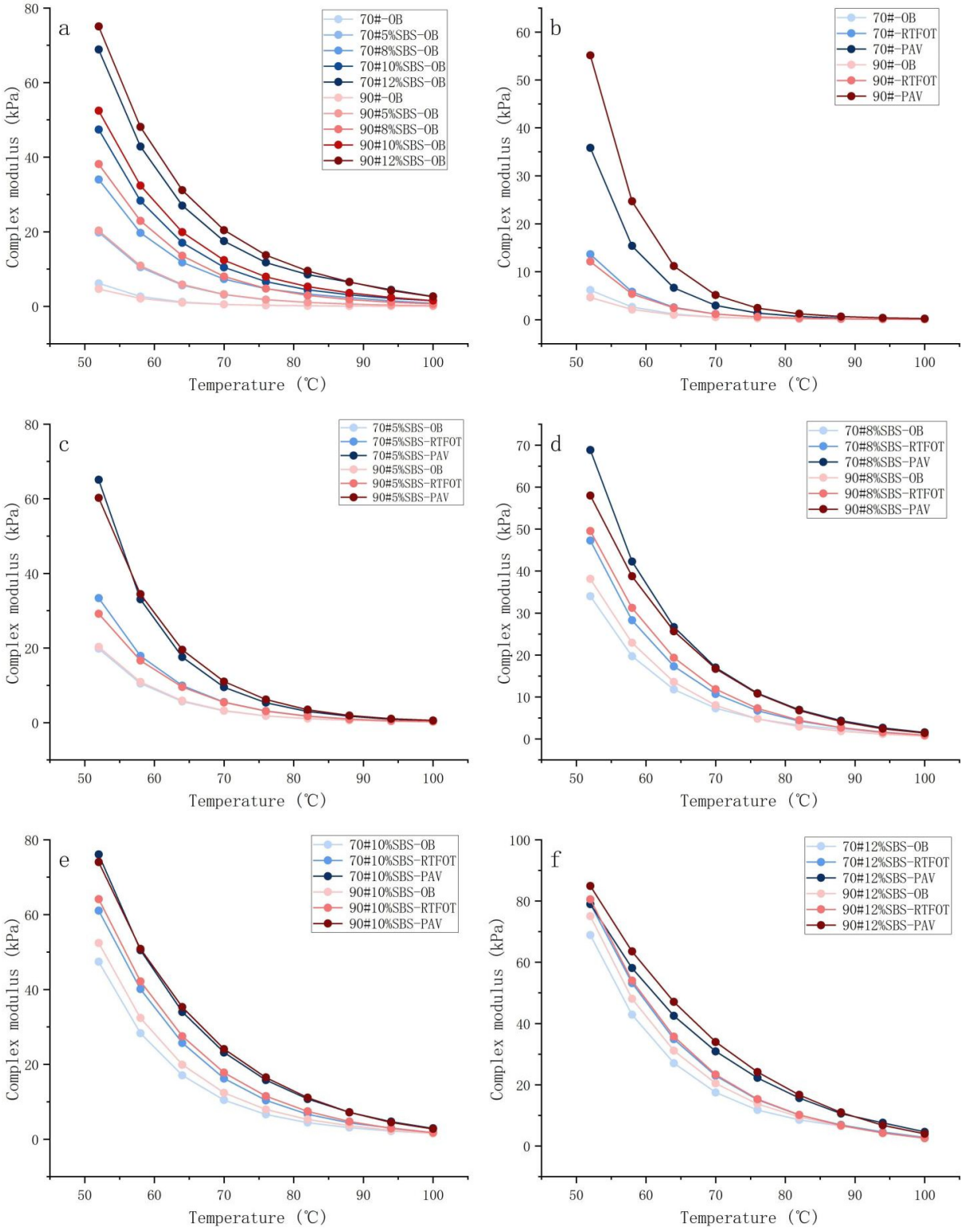

Figure 5. Complex modulus. (**a**) SBS-modified asphalt with different SBS contents (original state); (**b**) base asphalt under different aging states; (**c**) 5% SBS-modified asphalt under different aging states; (**d**) 8% SBS-modified asphalt under different aging states; (**e**) 10% SBS-modified asphalt under different aging states; (**f**) 12% SBS-modified asphalt under different aging states.

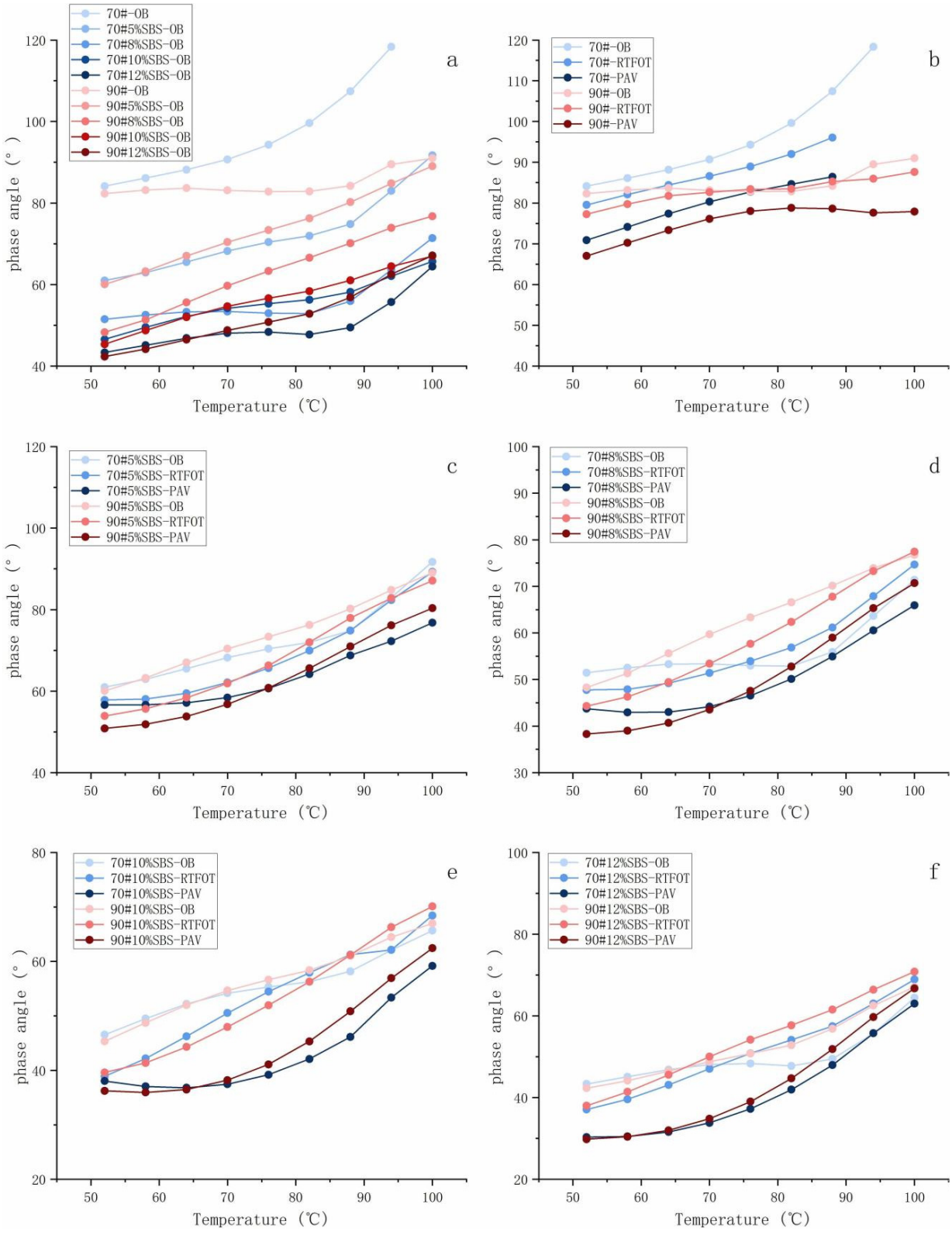

Figure 6. Phase angle. (**a**) SBS-modified asphalt with different SBS contents (original state); (**b**) Base asphalt under different aging states; (**c**) 5% SBS-modified asphalt under different aging states; (**d**) 8% SBS-modified asphalt under different aging states; (**e**) 10% SBS-modified asphalt under different aging states; (**f**) 12% SBS-modified asphalt under different aging states.

The test results showed that for unmodified asphalts, the δ value of 70# base asphalt was higher than that of 90# base asphalt in the temperature range of 52–75 °C, indicating

more significant viscous behavior of 70# base asphalt. However, when the temperature exceeded 76 °C, both types of base asphalts exhibited unusually high δ values greater than 90°. This phenomenon is attributed to the fact that the temperature sweep test was conducted at a strain amplitude of 12% (simulating actual loading conditions), which exceeds the LVE strain threshold (~3%) of unmodified asphalt. At high temperatures, the strength of base asphalt decreases sharply, and the 12% strain drives the material into the nonlinear viscoelastic region, leading to unusually high values of phase angle responses (e.g., δ > 90°) caused by plastic deformation and shear softening. In contrast, high-content SBS-modified asphalt has a higher LVE strain threshold (~5%), and the 12% strain still exceeds its LVE range at temperatures > 90 °C, but the three-dimensional elastic network formed by SBS inhibits excessive plastic deformation, resulting in no unusually high δ values.

After incorporating SBS, the δ values of both systems decreased with the increase in SBS content. For the 90#-based system, its δ value exceeded that of the 70#-based system in the high-temperature range while remaining lower in the low-temperature range (52 °C). The most significant decrease in δ was observed at 12% SBS content, confirming that the elastic network formed by high-content SBS enhances the "elasticity-dominated" characteristic of the material and exhibits a better regulatory effect on the viscosity of 70# base asphalt.

The influence of aging on δ was dependent on SBS content. At low SBS content (5%), the decrease in δ after PAV aging was much greater than that after RTFOT aging; at 70 °C, the ratio of δ decrease (PAV aging vs. RTFOT aging) for the 5% SBS system was < 1. At high SBS content (12%), the decrease in δ after PAV aging exceeded that after RTFOT aging, with the ratio > 1. This indicates that high-content SBS can strengthen the regulatory effect of aging on viscoelasticity. In addition, after PAV aging, the δ value of the 70#-based system was generally lower than that of the 90#-based system at high temperatures, reflecting a higher proportion of elasticity in 70# base asphalt after long-term aging. In contrast, 90# base asphalt retained more viscosity due to the easy oxidation of its aromatic components.

Increasing SBS content can optimize the viscoelastic balance of asphalt, but the regulatory mechanisms differ between different base asphalts. The 70# base asphalt requires an SBS content of 10–12% to achieve elasticity dominance, while the 90# base asphalt can significantly enhance elasticity at an SBS content of 8–10%.

3. Rutting Factor (G*/*sinδ)

The rutting factor is a key indicator of high-temperature rutting resistance (Figure 7), with specifications requiring ≥2.2 kPa for Performance Grade (PG) compliance [23]. Rutting factors of both base asphalts increased significantly with SBS content, and the 90#-based system had a greater increase than the 70#-based system at the same SBS content: 90# base asphalt's rutting factor surpassed 70# at 5% SBS, with the gap widening at ≥8% SBS. Aging's influence on the rutting factor depended on SBS content: at low SBS (5%), PAV aging caused a much larger increase in rutting factor than RTFOT aging (70#-based asphalt: 2.3× greater); at high SBS (12%), the difference between the two aging processes narrowed (70#-based system ratio: 1.1). PG classification showed that unmodified asphalts only reached PG64, 5% SBS increased the grade to PG76, and 8%, 10%, and 12% SBS reached PG88, PG94, and PG100, respectively—confirming that ≥8% SBS meets the needs of heavy-load, high-temperature scenarios (e.g., ultra-thin wearing courses).

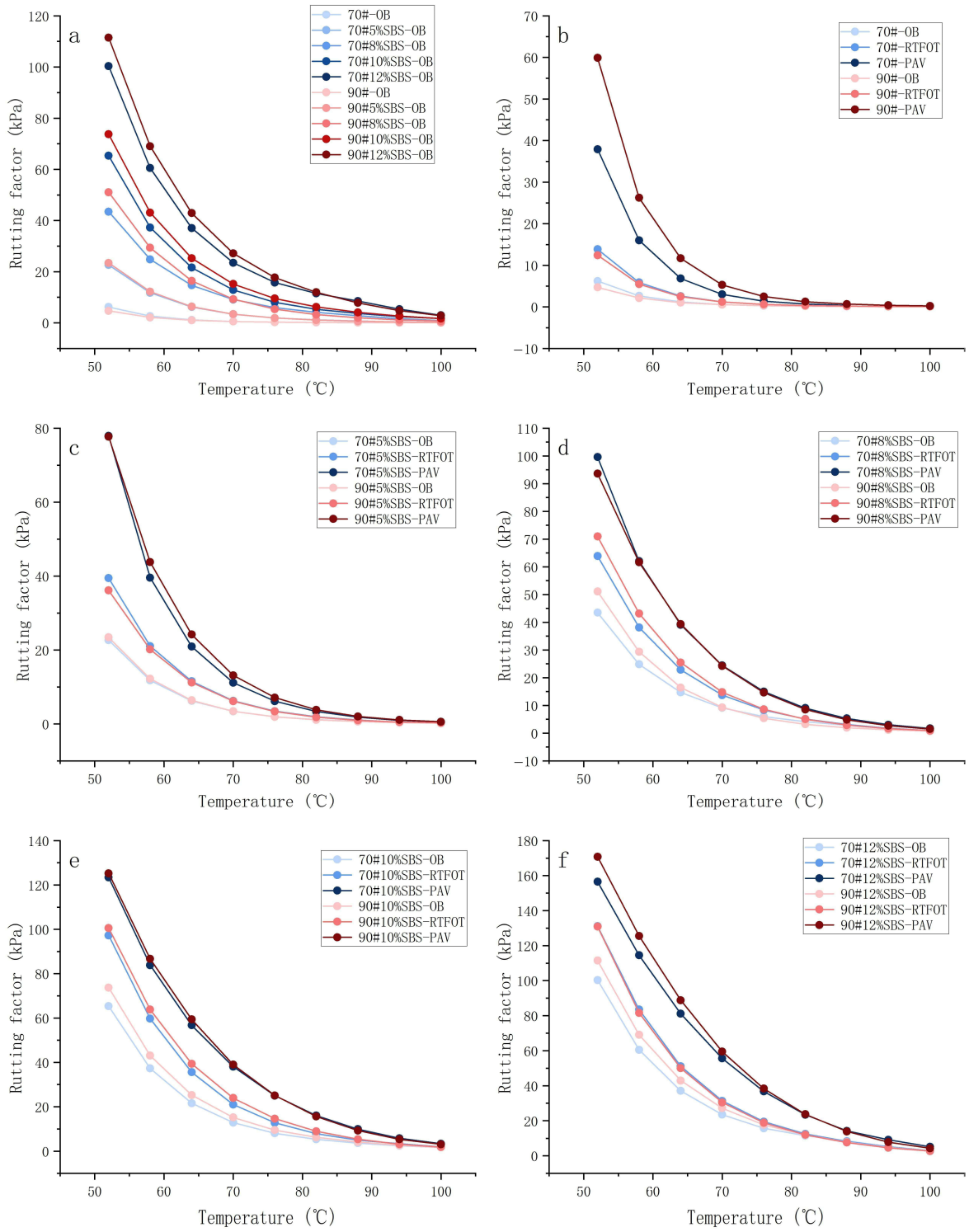

Figure 7. Rutting test and PG classification. (**a**) Modified asphalts with five different SBS contents: (**b**) 70# base asphalt; (**c**) 70# asphalt modified with 5% SBS; (**d**) 70# asphalt modified with 8% SBS; (**e**) 70# asphalt modified with 10% SBS; (**f**) 70# asphalt modified with 12% SBS.

3.5. Fatigue Characteristic Analysis

The fatigue factor (G*sinδ) is a core indicator characterizing the medium-temperature fatigue resistance of asphalt, directly reflecting the level of viscous energy dissipation of the material [24]. The result is shown in Figure 8. The test results showed that the fatigue factor increased with the increase in SBS content, which is attributed to the fact that the SBS modifier increases the viscosity of asphalt, thereby enhancing the viscous

contribution to the complex shear modulus. Without SBS addition, the fatigue factor of 90# base asphalt was lower than that of 70# base asphalt, indicating a higher proportion of elastic components in the 90# base asphalt. However, after incorporating SBS, the fatigue factor of the 90#-based system surpassed that of the 70#-based system, and the gap widened as the SBS content increased. This confirms that SBS has a more significant regulatory effect on the viscoelasticity of 90# base asphalt, which is related to the high content of light components in 90# base asphalt—these components facilitate the dispersion and cross-linking of SBS.

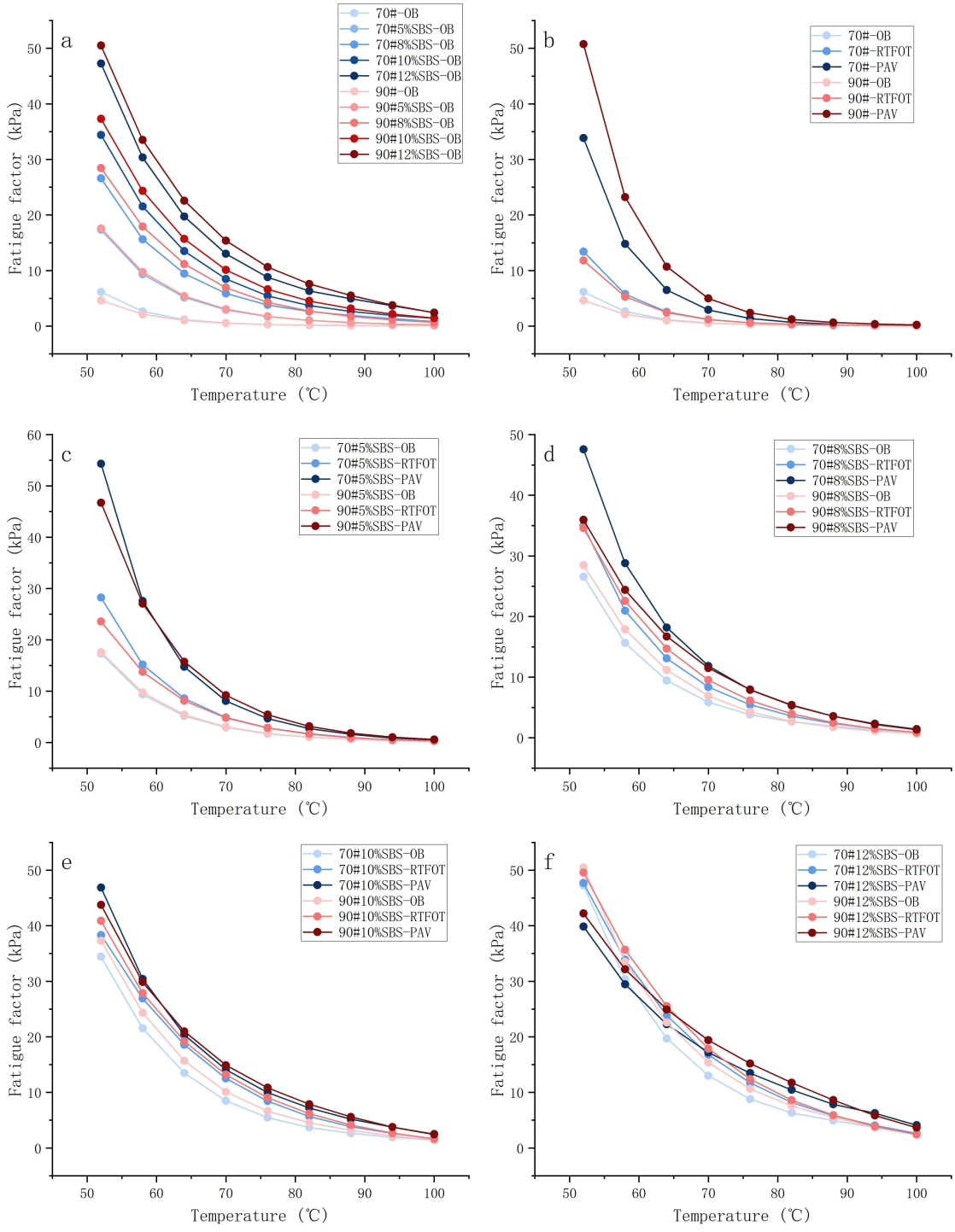

Figure 8. Fatigue factor. (**a**) 70# modified asphalts with five different SBS contents; (**b**) 70# base asphalt; (**c**) 70# asphalt modified with 5% SBS; (**d**) 70# asphalt modified with 8% SBS; (**e**) 70# asphalt modified with 10% SBS; (**f**) 70# asphalt modified with 12% SBS.

The influence of aging on the fatigue factor showed obvious dependence on SBS content. For SBS-modified asphalts with low content (≤10%), the fatigue factor increased significantly after RTFOT and PAV aging, leading to weakened fatigue resistance; notably, the impact of PAV aging was more prominent. In contrast, for the 12% SBS-modified asphalt, the fatigue factor decreased in some temperature ranges after PAV aging. This is presumably because, under the high-temperature and high-pressure conditions of PAV aging, the cross-linked structure of high-content SBS is damaged (resulting in reduced viscous components), or the material tends to exhibit elasticity-dominated characteristics at lower temperatures. In addition, with the increase in SBS content, the ratio of the fatigue factor increment from RTFOT to PAV aging to that from the original state to RTFOT aging gradually decreased; at 12% SBS content, this ratio even became negative. This fully demonstrates the excellent fatigue resistance and stability of high-content SBS-modified asphalt.

While the decrease in G*sinδ for 12% SBS asphalt post-PAV aging is favorable for medium-temperature fatigue resistance, this trend must be interpreted with caution to avoid overstating "improved fatigue resistance stability." As noted in Section 3.6, 12% SBS asphalt exhibits a viscosity decrease at 180 °C post-aging—attributed to partial SBS network disintegration under high temperature/pressure. This raises the possibility that the fatigue factor decrease is not solely a positive indicator of enhanced elasticity but may reflect a complex trade-off between residual network elasticity and incipient polymer degradation:

If the fatigue factor decrease were driven by embrittlement (e.g., severe SBS degradation), complementary indicators would show negative trends: (i) 5 °C ductility (low-temperature crack resistance) would decrease sharply, but our data shows 12% SBS asphalt retains 40.87 cm (70#) and 49.42 cm (90#) ductility post-PAV (only 8–10% reduction vs. original state); (ii) phase angle (δ) would drop below 40° (excessive rigidity), but δ remains 42–45° (Figure 6f)—indicating a balanced viscoelastic state, not embrittlement.

3.6. Viscosity Test

Rotational viscosity (135–180 °C) evaluated construction workability (Figure 9). Viscosity increased sharply with SBS content, especially at low temperatures: 70# asphalt's viscosity at 135 °C rose from 416 cP (base) to 27,500 cP (12% SBS, 66× increase), while 90# asphalt reached 24,150 cP (12% SBS). At 8% SBS, 70#-based asphalt had higher viscosity than 90#-based asphalt, but 90#-based asphalt surpassed it at ≥10% SBS (due to denser SBS networks from better light component dispersion).

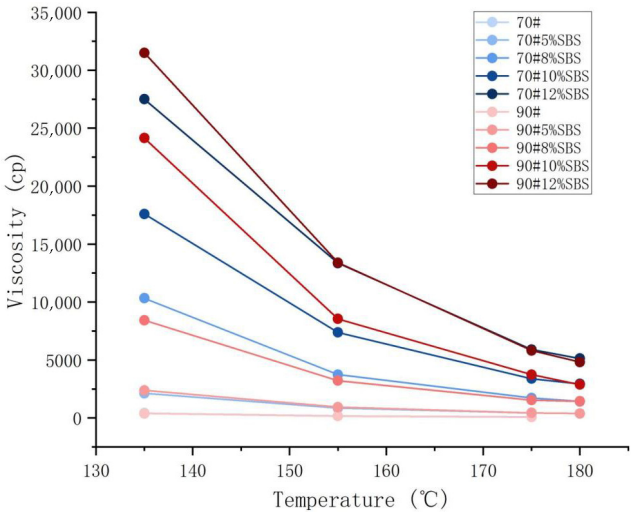

Figure 9. Viscosity of SBS-modified asphalts with different SBS contents.

Aging significantly increased viscosity. 70#-10% SBS asphalt had a 242% viscosity increase at 135 °C after PAV (vs. 49% after RTFOT). However, 12% SBS asphalt showed reduced viscosity at 180 °C after aging—likely due to SBS network disintegration under high temperature/pressure, 8%+ SBS asphalt exceeds the 135 °C viscosity limit, requiring construction temperatures >180 °C (balanced against potential aging risks) [25].

3.7. Viscoelastic Characteristic Analysis

Master curves of complex modulus simulate asphalt's viscoelastic behavior across temperatures and load durations (Figure 10), exhibiting a "wide left, narrow right" feature: curves shifted upward (higher stiffness), and the high-frequency/low-temperature slope decreased (reduced temperature sensitivity) with increasing SBS content and aging. Unmodified 70# base asphalt had a higher complex modulus than 90# in the high-frequency/low-temperature region, but the 90#-based system surpassed 70# at 8% SBS (high-frequency/low-temperature) and expanded its advantage at 10–12% SBS (52–94 °C)—attributed to better SBS network formation in 90#'s light components. Threshold differences existed between the two systems: 70#-based asphalt had a significant modulus increase at 10–12% SBS, while 90#-based asphalt had the largest increase at 8–10% SBS. Aging caused a gradual upward shift in master curves: unmodified 90# base asphalt's modulus surpassed 70# after PAV aging (oxidation of aromatic components), and at 12% SBS, the difference between RTFOT and PAV master curves narrowed—indicating the SBS network inhibits aging-induced structural degradation.

Viscoelastic characteristics determine asphalt's deformation resistance and stress relaxation capabilities under different temperatures and load durations—key for matching the diverse demands of the study's target applications. Master curves of complex modulus further clarify how high-content SBS achieves "optimal viscoelastic balance" for specific use cases:

For high-temperature heavy-load scenarios (e.g., ultra-thin wearing courses), the low-frequency/high-temperature region of the master curve (simulating slow, heavy loads at 60–70 °C) shows that 90#-10% SBS asphalt has a G* of 45 kPa—sufficient to resist permanent rutting (meets PG94 grade). Meanwhile, its $\delta = 48^\circ$ (Figure 6) avoids excessive rigidity, ensuring workability during compaction.

For medium-temperature fatigue scenarios (e.g., urban intersections), the medium-frequency/medium-temperature region (simulating repeated loads at 25–40 °C) shows that 70#-12% SBS asphalt has a G*sinδ (fatigue factor) of 2.8 kPa post-PAV aging—lower than the 3.5 kPa threshold for fatigue cracking, confirming optimal balance for fatigue resistance.

For low-temperature crack scenarios, the high-frequency/low-temperature region (simulating rapid thermal stress at −5–5 °C) shows that 70#–12% SBS asphalt has a G* of 100 MPa—lower than the 150 MPa threshold for brittle fracture, while its $\delta = 38^\circ$ retains enough viscosity to release thermal stress.

This application-specific optimization distinguishes high-content SBS from conventional SBS-modified asphalt (3–5% SBS), which typically only meets single-scenario requirements (e.g., rutting resistance but not fatigue resistance).

At the micro-mechanism level, the decreased slope of the master curve in the high-frequency/low-temperature region indicates that the material tends to be elasticity-dominated (excellent crack resistance); the larger slope in the low-frequency/high-temperature region reflects viscous flow characteristics (stress release capability) [26]. The 90# asphalt modified with 12% SBS exhibited stronger elasticity in the high-frequency/low-temperature region and more prominent viscosity in the low-frequency/high-temperature region, confirming its balanced characteristic of "low-temperature crack resistance and high-temperature rutting resistance". This result provides a quantitative viscoelastic basis

for the design of asphalt SBS content in different climate zones (e.g., high-temperature heavy-load zones, severe cold freeze–thaw zones).

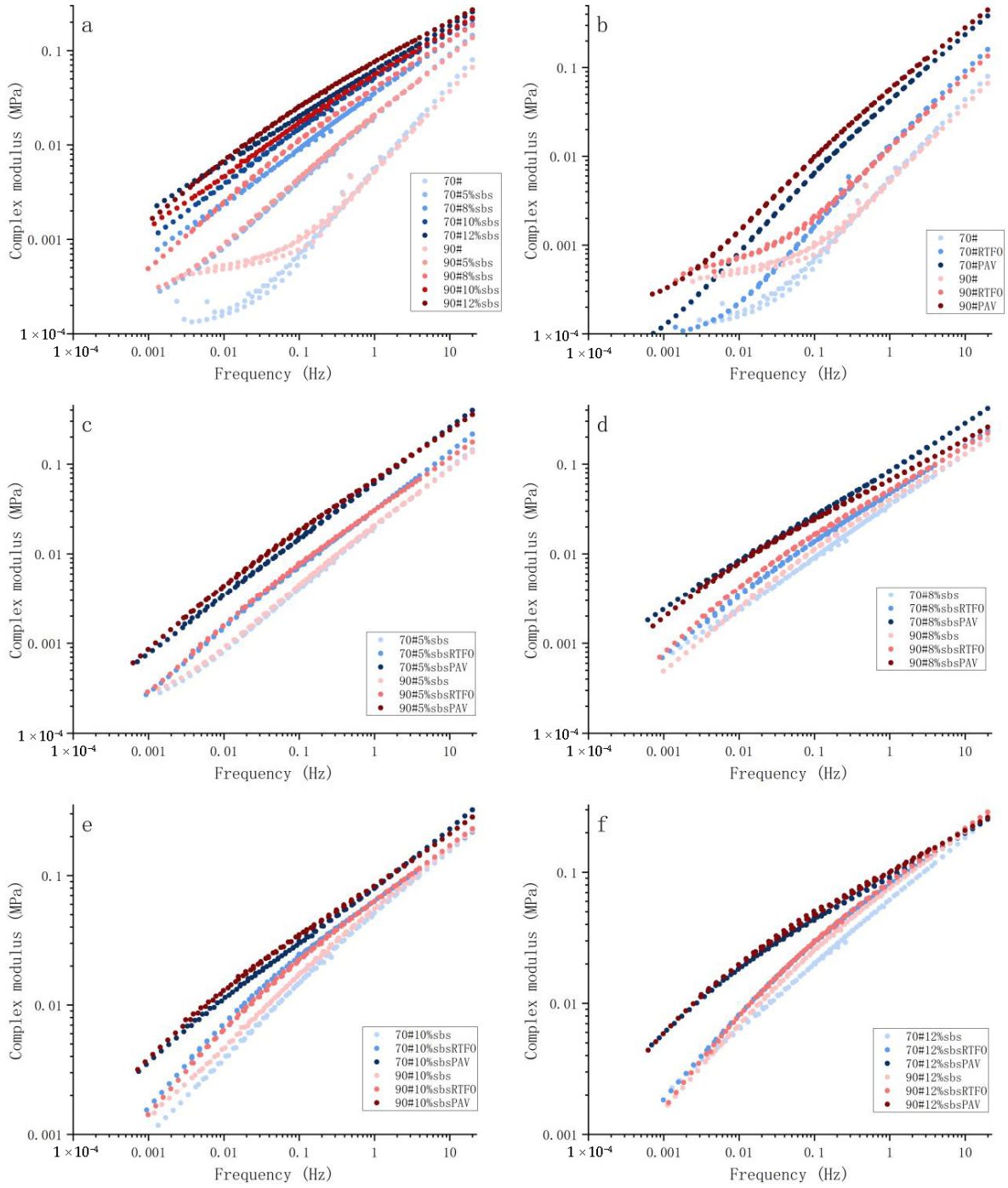

Figure 10. Main curve of the complex modulus of asphalt. (**a**) base binder; (**b**) aging binder; (**c**) asphalt modified with 5% SBS; (**d**) asphalt modified with 8% SBS; (**e**) asphalt modified with 10% SBS; (**f**) asphalt modified with 12% SBS.

3.8. Scanning Electron Microscopy (SEM) Analysis

SEM characterized the microstructure of asphalt with 0%, 5%, and 10% SBS at 500×, 1000×, and 5000× magnification (Figure 11), revealing gradient improvements with increasing SBS content. At 500×, 0% SBS base asphalt showed irregular strip-like undulations and rough particles (component distribution defects), 5% SBS improved surface flatness (pore filling by SBS), and 10% SBS formed a continuous, dense phase (network struc-

ture reconstruction). At 1000×, 0% SBS had aggregated particles and layered peeling (micro-defects), 5% SBS exhibited uniformly distributed SBS dispersed-phase dots (initial polymer-asphalt compatibility), and 10% SBS had no delamination or cracks (full SBS dispersion and strong interface bonding). At 5000×, 0% SBS had holes and collapses (loose microstructure), 5% SBS had a smooth surface with fine particles (initial polymer cross-linking), and 10% SBS had an extremely flat surface (nanoscale continuous SBS network). The increase in SBS content can gradually improve the microstructural defects of asphalt through a gradient effect of "pore filling → dispersion compatibility → network construction". The continuous and dense phase formed at 10% SBS content is the key to the significant improvement of high-temperature deformation resistance and low-temperature crack resistance.

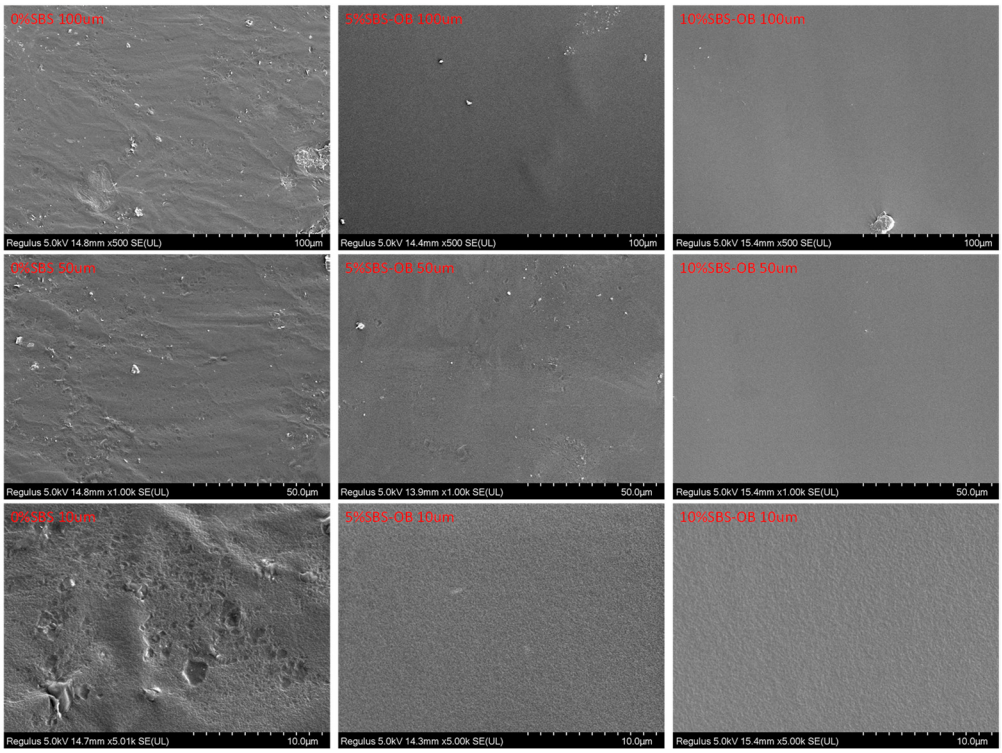

Figure 11. SEM images of asphalt with different SBS content.

3.9. X-Ray Photoelectron Spectroscopy (XPS) Analysis

XPS quantified surface elemental composition (C, O, S) of 70# base asphalt and its 5%/10% SBS-modified counterparts under original, RTFOT, and PAV aging states (Figure 12). Carbon content (core organic component) decreased with aging: 70# base asphalt's C content dropped from 89.31% (original) to 69.15% (PAV), while 10% SBS-modified asphalt's C content only dropped to 74.13% (PAV)—indicating the SBS network inhibits light component loss. Oxygen content (oxidation degree indicator) increased with aging: 70# base asphalt's O content rose from 5.2% (original) to 22.67% (PAV), while 10% SBS-modified asphalt's O content only reached 17.86% (PAV)—the SBS network blocks oxygen penetration and reduces oxidative product formation. Sulfur content (sulfide stability indicator) decreased in low-content SBS systems (5% SBS: 1.88% original → 1.19% PAV) but slightly increased in high-content systems (10% SBS: 1.61% original → 1.84% PAV)—the SBS network restricts sulfide migration and may induce cross-linking reactions. XPS confirms that high-content SBS enhances asphalt's anti-aging ability from an elemental perspective.

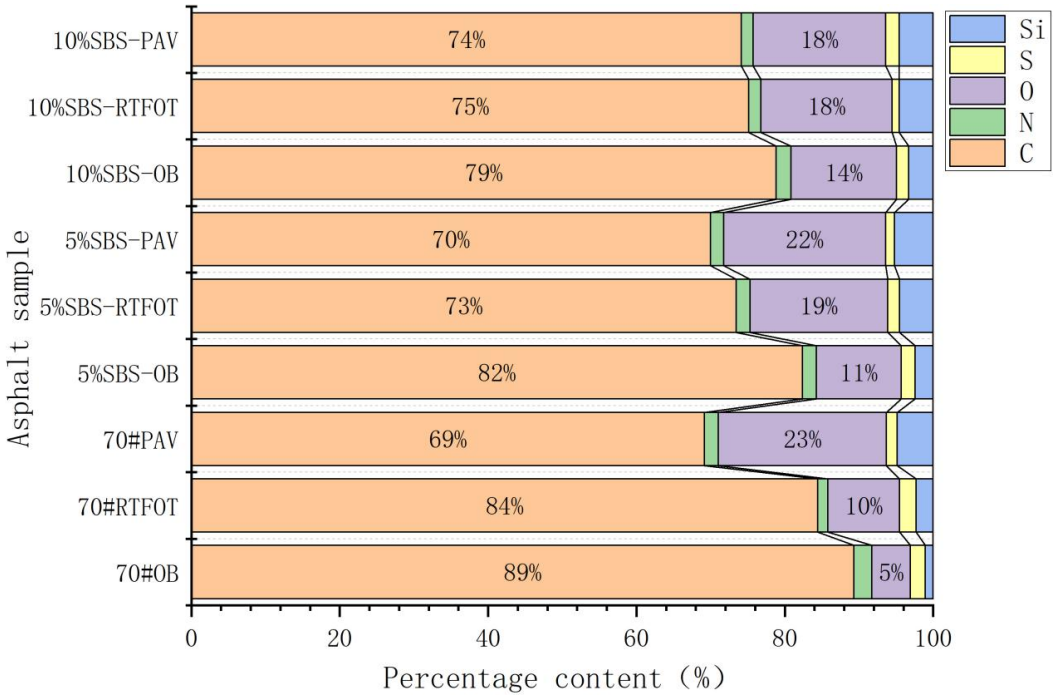

Figure 12. XPS element ratio.

XPS analysis confirmed that high-content SBS can enhance the anti-aging ability of asphalt from the elemental perspective by inhibiting C loss, slowing O intake, and stabilizing S form. Due to its higher content of light components, the 90# base asphalt showed a greater variation in elemental content than the 70# base asphalt, requiring a higher SBS content to achieve performance balance. This result provides a quantitative basis at the surface chemical level for the design of anti-aging formulas for modified asphalt.

4. Conclusions

This study systematically investigated the performance and aging behavior of high-content SBS-modified asphalt (5–12% SBS) using 70#/90# base asphalts, combining macro-performance tests, rheological analysis, and micro-characterization. The key findings and implications are summarized as follows:

1. High-content SBS synergizes with base asphalt type to enhance multi-scenario performance: SBS content (5–12%) and base asphalt type jointly determine asphalt performance. 90# base asphalt (higher light components) achieves better modification effects, with 12% SBS yielding 5 °C ductility (49.42 cm, 8× higher than unmodified) and 60 °C complex shear modulus (41.62 kPa, 77× higher than unmodified). 70# base asphalt requires 10–12% SBS to reach similar low-temperature performance, while 90# base asphalt achieves elasticity dominance at 8–10% SBS. Both systems upgrade from PG64 (unmodified) to PG100 (12% SBS), meeting heavy-load/high-temperature demands (e.g., ultra-thin wearing courses).
2. High-content SBS optimizes viscoelastic balance and inhibits aging via microstructural regulation. At the macroscale, 10–12% SBS adjusts phase angle (δ) to 40–45° (elasticity-dominated for fatigue resistance) and reduces PAV-aged fatigue factor (G*sinδ) in 60–70 °C—avoiding embrittlement (evidenced by 8–10% ductility retention). At the microscale, 10% SBS forms a continuous dense network (SEM), while XPS confirms it inhibits carbon loss (C content reduction <8% post-PAV vs. 22% for unmodified) and slows oxygen incorporation (O content increase <18% post-PAV vs. 23% for unmodified), enhancing anti-aging durability.

3. Practical application requires balancing high performance with construction feasibility. 12% SBS asphalt exhibits ultra-high viscosity (27,500 cP at 135 °C), necessitating construction temperatures >180 °C—though this induces more severe short-term aging (12.7% additional penetration reduction vs. standard RTFOT) and increases energy costs by ~23%. Mitigation strategies include adding 0.3% warm-mix additives (lowering construction temperature to 170 °C) or optimizing SBS content regionally (10% SBS for high-temperature areas, 12% SBS only for severe cold regions).
4. A critical SBS content threshold (8%) exists: below 8%, SBS acts as a dispersed phase (steep penetration reduction, +13–17 percentage points per 3% SBS); above 8%, it forms a continuous network (slowed reduction, +7–12 percentage points per 2% SBS). This threshold, combined with base asphalt type, provides a quantitative basis for formula design (e.g., 90# + 8–10% SBS for high-temperature heavy-load zones; 70# + 10–12% SBS for cold regions).

Author Contributions: Conceptualization, Q.Z. and H.W.; methodology, S.Y.; software, Q.Z.; validation, B.J. and T.W.; formal analysis, S.Y.; investigation, Q.Z.; resources, T.W.; data curation, H.W.; writing—original draft preparation, B.J.; writing—review and editing, Q.Z.; visualization, T.W.; supervision, H.W.; project administration, Q.Z.; funding acquisition, T.W. All authors have read and agreed to the published version of the manuscript.

Funding: This research was supported by the Fundamental Research Funds for the Central Universities (No. 2025JBMC032).

Data Availability Statement: The original contributions presented in this study are included in the article. Further inquiries can be directed to the corresponding author.

Conflicts of Interest: The authors declare no conflicts of interest.

References

1. Yan, C.; Huang, W.; Lin, P.; Zhang, Y.; Lv, Q. Chemical and rheological evaluation of aging properties of high content SBS polymer modified asphalt. *Fuel* **2019**, *252*, 417–426. [CrossRef]
2. Li, Y.; Ma, R.; Wang, X.; Cheng, P.; Chen, Y. Improvement effect of different modifiers on storage stability of high content SBS modified asphalt. *Case Stud. Constr. Mater.* **2024**, *20*, e02820. [CrossRef]
3. Yuan, D.; Xing, C.; Jiang, W.; Xiao, J.; Wu, W.; Li, P.; Li, Y. Viscoelastic behavior and phase structure of high-content SBS-modified asphalt. *Polymers* **2022**, *14*, 2476. [CrossRef]
4. Wu, W.; Cavalli, M.C.; Jiang, W.; Kringos, N. Differing perspectives on the use of high-content SBS polymer-modified bitumen. *Constr. Build. Mater.* **2024**, *411*, 134433. [CrossRef]
5. Lin, P.; Yan, C.; Huang, W.; Li, Y.; Zhou, L.; Tang, N.; Xiao, F.; Zhang, Y.; Lv, Q. Rheological, chemical and aging characteristics of high content polymer modified asphalt. *Constr. Build. Mater.* **2019**, *207*, 616–629. [CrossRef]
6. Wang, T.; Weng, Y.; Cai, X.; Li, J.; Xiao, F.; Sun, G.; Zhang, F. Statistical modeling of low-temperature properties and FTIR spectra of crumb rubber modified asphalts considering SARA fractions. *J. Clean. Prod.* **2022**, *374*, 134016. [CrossRef]
7. Yan, C.; Huang, W.; Ma, J.; Xu, J.; Lv, Q.; Lin, P. Characterizing the SBS polymer degradation within high content polymer modified asphalt using ATR-FTIR. *Constr. Build. Mater.* **2020**, *233*, 117708. [CrossRef]
8. tur Rasool, R.; Hongru, Y.; Hassan, A.; Wang, S.; Zhang, H. In-field aging process of high content SBS modified asphalt in porous pavement. *Polym. Degrad. Stab.* **2018**, *155*, 220–229. [CrossRef]
9. Zhang, J.; Huang, W.; Hao, G.; Yan, C.; Lv, Q.; Cai, Q. Evaluation of open-grade friction course (OGFC) mixtures with high content SBS polymer modified asphalt. *Constr. Build. Mater.* **2021**, *270*, 121374. [CrossRef]
10. Lin, P.; Huang, W.; Liu, X.; Apostolids, P.; Wang, H.; Yan, C. Laboratory evaluation of the effects of long-term aging on high-content polymer-modified asphalt binder. *J. Mater. Civ. Eng.* **2020**, *32*, 04020157. [CrossRef]
11. Nie, X.; Li, Z.; Yao, H.; Hou, T.; Zhou, X.; Li, C. Waste bio-oil as a compatibilizer for high content SBS modified asphalt. *Pet. Sci. Technol.* **2020**, *38*, 316–322. [CrossRef]
12. Zheng, K.; Xu, J.; Wang, J. Viscoelasticity of recycled asphalt mixtures with high content reclaimed SBS modified asphalt pavement. *Sustainability* **2023**, *15*, 2515. [CrossRef]
13. Wang, T.; Wei, X.; Zhang, D.; Shi, H.; Cheng, Z. Evaluation for low temperature performance of SBS modified asphalt by dynamic shear rheometer method. *Buildings* **2021**, *11*, 408. [CrossRef]

14. Li, Y.; Li, J.; Yang, H.; Ye, Z.; Hu, C.; Shen, S. Laboratory evaluation of synergistic blending with SBS-modified bitumen and rejuvenator to enhance the performance of recycled bitumen with a high content of RAP materials. *Constr. Build. Mater.* **2024**, *442*, 137675. [CrossRef]
15. Lin, P.; Liu, X.; Ren, S.; Xu, J.; Li, Y.; Li, M. Effects of bitumen thickness on the aging behavior of high-content polymer-modified asphalt mixture. *Polymers* **2023**, *15*, 2325. [CrossRef]
16. Li, Y.; Ma, R.; Cheng, A.; Huang, X.; Cheng, P.; Gao, Q.; Chen, X. Study on the construction of storage stability master curve and evaluation methods of high content SBS modified asphalt under thermal time coupling effect. *Constr. Build. Mater.* **2025**, *494*, 143409. [CrossRef]
17. Dong, F.; Wan, L.; Shi, J.; Yu, X.; Jin, Y.; Zhou, Y.; Chen, J.; Xu, Z. Functional Design of Warm Mix Additives and its Influence on the Performance of High-Content SBS-Modified Asphalt. *Case Stud. Constr. Mater.* **2025**, *23*, e05267. [CrossRef]
18. Yan, C.; Huang, W.; Lv, Q.; Lin, P. Investigating the field short-term aging of high content polymer-modified asphalt. *Int. J. Pavement Eng.* **2021**, *22*, 1263–1272. [CrossRef]
19. Xu, S.; Fan, Y.; Feng, Z.; Ke, Y.; Zhang, C.; Huang, H. Comparison of quantitative determination for SBS content in SBS modified asphalt. *Constr. Build. Mater.* **2021**, *282*, 122733. [CrossRef]
20. Lin, P.; Liu, X.; Ren, S.; Li, Y.; Xu, J.; Li, M. Unraveling the influence of fibers on aging susceptibility and performance of high content polymer modified asphalt mixtures. *Case Stud. Constr. Mater.* **2023**, *18*, e02211. [CrossRef]
21. Jing, W.; Ding, S.; Wang, L.; Lu, W.; Ge, D. Performance evaluation of styreneic methyl copolymer regenerated SBS-modified asphalt and its mixture with high content RAP. *Case Stud. Constr. Mater.* **2023**, *19*, e02657. [CrossRef]
22. Su, Q.; Xia, L.; Tang, J.; Zhang, M.; Wang, D.; Cao, D. From waste tires to long-life asphalt pavement: Evaluation of rheological and fatigue properties of high-content rubber/SBS composite modified asphalt. *Constr. Build. Mater.* **2025**, *495*, 143671. [CrossRef]
23. Yao, H.; Wang, Q.; Zhang, Z.; Zhou, X.; Cao, Y. Effect of styrene–butadiene–styrene triblock copolymer structure on the rheological properties of high content SBS polymer modified asphalts. *Constr. Build. Mater.* **2023**, *400*, 132738. [CrossRef]
24. Han, D.; Hu, G.; Zhang, J. Study on anti-aging performance enhancement of polymer modified asphalt with high linear SBS content. *Polymers* **2023**, *15*, 256. [CrossRef] [PubMed]
25. Pei, Y.; Jiang, S.; Ding, Z.; Cheng, L.; Li, P.; Jiang, X. Preparation and performance analysis of high-viscosity asphalt containing high-content SBS and crumb rubber by oxygen-free high-temperature treatment. *Constr. Build. Mater.* **2023**, *402*, 132763. [CrossRef]
26. Wu, W.; Jiang, W.; Xiao, J.; Yuan, D.; Wang, T.; Ling, X. Investigation of LAS-based fatigue evaluation methods for high-viscosity modified asphalt binders with high-content polymers. *Constr. Build. Mater.* **2024**, *422*, 135810. [CrossRef]

Disclaimer/Publisher's Note: The statements, opinions and data contained in all publications are solely those of the individual author(s) and contributor(s) and not of MDPI and/or the editor(s). MDPI and/or the editor(s) disclaim responsibility for any injury to people or property resulting from any ideas, methods, instructions or products referred to in the content.